Asymmetric disassembly and robustness in declining networks

Serguei Saavedra*, Felix Reed-Tsochas†‡, and Brian Uzzi§

*Department of Engineering Science and CABDyN Complexity Centre, Oxford University, Oxford OX1 3PJ, United Kingdom; †James Martin Institute and CABDyN Complexity Centre, Saïd Business School, Oxford University, Oxford OX1 1HP, United Kingdom; and §Kellogg School of Management and Northwestern Institute on Complex Systems, Northwestern University, Evanston, IL 60208

Edited by Simon A. Levin, Princeton University, Princeton, NJ, and approved September 3, 2008 (received for review May 17, 2008)

Mechanisms that enable declining networks to avert structural collapse and performance degradation are not well understood. This knowledge gap reflects a shortage of data on declining networks and an emphasis on models of network growth. Analyzing >700,000 transactions between firms in the New York garment industry over 19 years, we tracked this network's decline and measured how its topology and global performance evolved. We find that favoring asymmetric (disassortative) links is key to preserving the topology and functionality of the declining network. Based on our findings, we tested a model of network decline that combines an asymmetric disassembly process for contraction with a preferential attachment process for regrowth. Our simulation results indicate that the model can explain robustness under decline even if the total population of nodes contracts by more than an order of magnitude, in line with our observations for the empirical network. These findings suggest that disassembly mechanisms are not simply assembly mechanisms in reverse and that our model is relevant to understanding the process of decline and collapse in a broad range of biological, technological, and financial networks.

complex networks | contraction | socioeconomic systems

Research on the dynamics and robustness of complex networks (1–3) has emphasized the study of global network growth, identifying assembly mechanisms such as preferential attachment (4, 5), vertex fitness (6), vertex duplication (7), and fractal network growth (8), which, at the macroscopic level, generate stable topological characteristics despite large fluctuations in the microscopic network parameters. In addition, mechanisms have been proposed that can produce stable topological metrics in networks of constant size (9–12). Notably, methods based on percolation theory have significantly contributed to our understanding of how robust the static network structures generated by these assembly mechanisms are to fragmentation under random and targeted attack (8, 13–15).

Less is known about the dynamics and robustness of networks under sustained decline. In declining networks, new nodes and links may be added over time but the net process is a progressive loss of nodes and links. Hence, although assembly mechanisms may come into play, the emphasis must be on which disassembly mechanisms help preserve the topological characteristics and performance of the network. For example, Alzheimer's research examines how degradation in mental performance can be related to the progressive loss and disconnection of neurons with age (16). In an ecological context, analogous questions arise regarding the vulnerability of food webs to habitat loss and fragmentation (17, 18). In social and economic systems, network decline has raised questions about the preservation of social capital (19), resource allocation in developing economies (20), the prevention of financial collapse (21), effective coordination among suppliers (22), the restructuring of political systems (23), and lock-in into inferior technological standards (24).

We analyze the interorganizational network that makes up the famous New York City Garment Industry (NYGI) (25, 26), which has persistently shrunk over the last 19 years. In this network, nodes correspond to designers and contractors that are linked through coproductions of annual runs of lines of clothing. Designers design clothing and contractors fabricate it, but their roles often overlap because the industry's low-cost and quick-to-market conditions entwine design and production (25, 27). Our data include virtually all 10,000 plus firms and their >700,000 bilateral exchanges, circa 1985–2003, as recorded by the Union of Needle Trades and Industrial and Textile Employees (UNITE) (see *Methods*). Although these data resemble nation-to-nation commodity flow or interbank payment data (28–31), there are important differences. The links are not directional as in commodity chains, which are typified by flows from raw to finished goods along distinct stages of production. Instead, in our data, links are primarily reciprocal. They reflect the coproduction process between designers and contractors at one stage in the production process. Also, we have a measure of network performance not found in trade data: the fraction of bilateral transactions with errors per annum, which directly gauges the network's loss of functionality.

In this article, we show that the topological robustness of a declining network depends critically on how disassembly and assembly processes act in conjunction with each other. We define topological robustness as the ability of a network subject to both contraction and growth processes to resist quick fragmentation and to preserve the stability of key metrics characterizing the network topology. Our analysis and model indicates that in a declining network the growth process corresponding to partial recovery follows preferential attachment (PA) (4), and the contraction process favors the preservation of asymmetric links (namely, interactions between high-degree nodes and low-degree nodes). We label this contraction process asymmetric disassembly and show that it is associated with stable topological and functional features in a declining network. Song *et al.* (8) showed that for growing networks disassortativity generates self-similar structures that play a crucial role in preventing network fragmentation. Our model complements these findings by identifying disassembly mechanisms that avert network fragmentation in a distinct class of network problems corresponding to sustained decline.

Empirical Results and Discussion

Topological robustness and network contraction. The starting point for our analysis charts changes in the topology and performance

Author contributions: F.R.-T. designed research; S.S., F.R.-T., and B.U. performed research; S.S., F.R.-T., and B.U. analyzed data; S.S., F.R.-T., and B.U. wrote the paper; and B.U. provided access to a new dataset.

The authors declare no conflict of interest.

This article is a PNAS Direct Submission.

‡To whom correspondence should be addressed. E-mail: felix.reed-tsochas@sbs.ox.ac.uk.

This article contains supporting information online at www.pnas.org/cgi/content/full/0804740105/DCSupplemental.

Table 1. Decline and stable topological properties of the network

Year	*LCC* (%)	*L*	$\langle k \rangle$	$\langle l \rangle$	*D*	α	k_{min}	k_{max}	ν
1985	3,249 (95)	7,250	4.46	4.22	14	2.44	4	50	−0.52
1988	2,410 (94)	5,504	4.56	4.16	12	2.38	4	47	−0.49
1991	1,880 (93)	3,981	4.23	4.15	11	2.31	4	56	−0.55
1994	1,135 (93)	1,917	3.37	4.3	10	2.36	3	48	−0.52
1997	842 (91)	1,450	3.44	4.06	10	2.38	4	54	−0.55
2000	449 (87)	716	3.18	4.01	9	2.20	2	—	−0.54
2003	190 (84)	228	2.4	4.07	10	2.09	1	—	−0.56

LCC represents the total number of firms in the network's largest connected component along with the observed percentage in parentheses of the LCC in the empirical network, *L* gives the number of connections in the LCC, $\langle k \rangle$ is the average number of connections per firm in the network, $\langle l \rangle$ is the average path length, and *D* is the diameter of the network (maximum distance between two firms). Here α, k_{min}, and k_{max} correspond to the power-law exponent and the minimum and maximum cut-off values respectively, where the function $P_{cum}(k) = (k)^{-(\alpha-1)}$ is validated by the Kolmogorov–Smirnov goodness-of-fit test and following Newman (42) for the calculations (see *SI Text*, section 1). Finally, the table shows the exponent ν of the nearest-neighbors average connectivity of nodes degree *k* as defined by $\langle k_{nn} \rangle_k \sim k^{\nu}$.

of the NYGI network as it shrinks in size [see supporting information (SI) Fig. S1 and Table S1]. The findings suggest that in a declining network, topological robustness can be preserved despite massive turnover and a substantial net loss of nodes and links. The persistence of topological robustness as the network evolves coincides with a stable measure of network performance.

Topological changes were measured with characteristics that focus on the network's connectivity and degree distribution and that have been used in prior research on network dynamics (32). Table 1 shows the observed contraction of the largest connected component (LCC) and total number of links *L*, and the progressive decline in the average degree $\langle k \rangle$ of nodes. However, as shown in Table 1, the LCC resisted fragmentation in the sense that it contained a high and relatively stable proportion of the total nodes within the empirical network over the years. Focusing on the network's topological features, Table 1 also shows that the average path length $\langle l \rangle$ and diameter *D* of the network remain stable. The degree distribution is characterized by a truncated power-law and remains stable over the observation period, until 2000, when finite size effects in the network become stronger (see Table 1 and Fig. S2). Fig. 1*A* shows how the cumulative degree distribution $P_{cum}(k)$ varies over the observation period, where for a given year the distribution is calculated using all transactions in that year (see *SI Text* and Table S2). In addition, we track over time how the average over the degree of all nodes $\langle k_{nn} \rangle$ directly connected to a reference node *k* scales with the degree of that node (32). As shown in Fig. 1*B*, we find that this relation is defined by $\langle k_{nn} \rangle_k \sim k^{\upsilon}$ with $\upsilon \approx -0.5$ (see Table 1), which provides strong evidence for disassortativity (i.e., preference of high-degree nodes to connect to low-degree nodes and vice versa) (32) and the persistence of topological features in the network (see also Figs. S3 and S4). Disassortativity is common in biological, technological and financial networks (8, 29, 33, 34), which suggests that asymmetric links may play an important role in network robustness.

To measure changes in performance directly, we examine the network's error rate, given by the fraction of bilateral transactions that include "refunds." A refund is a reversal of a transaction between firms that occurs when the original exchange involved an error (e.g., design mistakes, shorted goods, manufacturing errors, etc.). A low fraction of errors signifies high performance. Fig. 1*C* shows how refunds as a percentage of total transactions changed each year over the observation period. We see that the fraction of links with errors remained reasonably stable until 1998, after which its mean and variability rose significantly. The observed correspondence between changes in the network topology and functional performance suggest that assembly and disassembly mechanisms, structure, and function are strongly related (see *Methods*).

Assembly and Disassembly Mechanisms. Building on prior research on the growth and cohesiveness of social networks (35, 36), we first analyze the data to see whether local assembly rules for nodes during global decline follow PA mechanisms. PA assumes that a node's degree provides a reasonable proxy measure for its fitness when direct performance information is unavailable for nodes (38, 37). In this way, a node's probability of acquiring new links is linearly proportional to its degree (fitness). We found that newcomer firms enter with low degree (see Fig. S5), and, consistent with past research, PA characterizes how newcomer firms attach to incumbent firms. Fig. 2*A* shows the relative probability $T_k(t)$, compared with random firm selection, that a link added at year *t* connects to an incumbent firm with $k(t-1)$ previous partners. This probability is defined by $T_k(t) \sim k(t)^{\nu}$ with $\nu = 1.20 \pm 0.06$ ($R^2 = 0.81$), which shows that the number of newcomers' links acquired by incumbent firms scales proportionally with the firms' degree (39).

Shifting our focus to deletion mechanisms for nodes, we found that firms have a probability of deletion inversely proportional to their degree (see Fig. S6), in line with realistic deletion mechanisms found in other dynamic networks (40, 41). Given that the mechanism acting on newcomer nodes that is responsible for the partial growth process mirrors the mechanism by which nodes are deleted as part of the contraction process, we examine whether contraction and recovery processes for links between incumbent nodes follow the same pattern.

Following this logic, we measure the relative probabilities $R_k^-(t)$ and $R_k^+(t)$ that an incumbent firm with *k* links in year $t-1$ will lose and gain new incumbents' links in year t (i.e., excluding newcomer attachment). We again followed Newman (39) to extract $R_k^+(t)$, and found that a firm's relative probability, compared with random firm selection, of gaining new links by connecting to other incumbent firms scales with the firm's degree as $R_k^+(t) \sim k(t)^{\nu}$ with $\nu = 0.84 \pm 0.04$ ($R^2 = 0.72$) (see Fig. S7). For the relative probability of link deletion, we calculate $R_k^-(t)$, assuming that links are randomly removed between incumbent firms. Fig. 2*B* shows that the probability of a firm losing a link decreases in proportion to the firms' degree as $k(t)^{\nu}$ with $\nu = -0.41 \pm 0.04$ ($R^2 = 0.54$) and a significant exception for the least connected firms. Our statistical analysis for links shows that PA seems to explain the assembly rule, whereas the disassembly rule is characterized by an asymmetric process that favors firms with extreme low and high degrees.

Considering our results on assembly and disassembly rules for links in the context of socioeconomic networks, differences in the nature of the information available to firms creating new links or breaking existing links may account for the observed assembly and disassembly mechanisms. In assembly, the use of a firm's degree as a proxy for fitness when forming new links

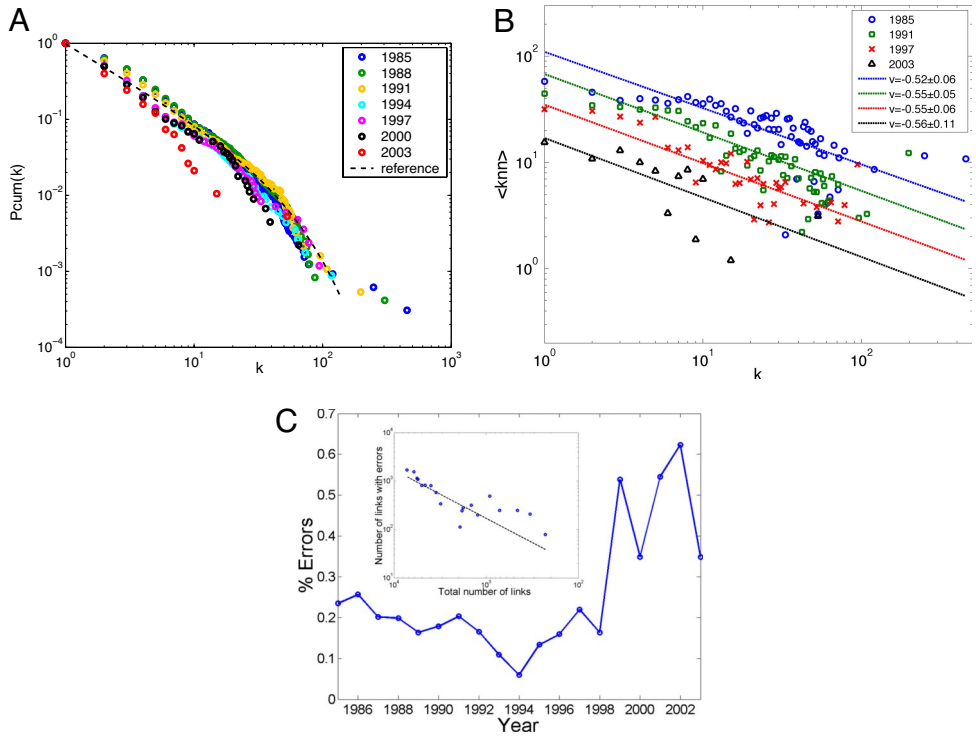

Fig. 1. Topological stability. (*A*) We observe a stable cumulative distribution from 1985 to 1999 characterized by a broad-scale distribution over two orders of magnitude on a log-log scale. The period 2000–2003 becomes noisy due to the small size of the network (see also Fig. S2). The reference line corresponds to a truncated power law defined by $P_{\text{cum}}(k) = k^{-(\alpha-1)}\, e^{\frac{-k}{k_{\max}}}$ with $\alpha = 2.3$ and cut-off $k_{\max} = 50$. The deviating points in the tail of the distributions all correspond to the idiosyncratic behavior of a single firm. (*B*) Disassortativity. Following Vázquez *et al.* (32) we calculated the disassortativity of the network by the nearest-neighbor average connectivity $\langle k_{\text{nn}} \rangle_{\text{k}} = \Sigma_{k'} k' P_{\text{c}}(k'|k)$ of nodes with connectivity k, where $P_{\text{c}}(k'|k)$ is the conditional probability that a link belonging to a node degree k connects to a node degree k'. The figure presents on a log-log scale the disassortativity for the network configuration in 1985 (blue circles), 1991 (green squares), 1997 (red crosses), and 2003 (black triangles). Dashed lines represent the fit to the data defined by $\langle k_{\text{nn}} \rangle_k \sim k^{\upsilon}$ where $\upsilon \approx -0.5$. Note that in 2003 the correlation becomes noisy (see also Fig. S3). (*C*) The figure shows the percentage of links with errors or refunds for each year. Note the increase in errors from 1999 to 2003. (Inset) Correlation between the total number of links (*x* axis) in descending order and the number of links with errors (*y* axis) for each year on a log–log scale. The dashed line corresponds to the average error rate of 18%, which characterizes most of the observation period. The deviations at the tail show that the increase in the error rate in 1999–2003 is not a simple result from the fluctuations in the total number of links.

makes sense because gathering direct performance data are costly when there is no existing link that can act as a conduit for quality information. By contrast, during disassembly there is already a link in place. Through this link the quality of a trading relationship can be judged based on firm-specific, first-hand information taking into account the history of past interactions. Because disassembly decisions can be based on direct data from "the horse's mouth" rather than a proxy, the degree—a general index of a node's fitness—is less valuable than the firm-specific information garnered through a link. This means that the lowest degree firms could be excellent collaborators who have become well adapted to an exclusive, high-quality relationship, an argument supported by field work that has found that asymmetric links are indicative of good working partnerships in competitive markets like the NYGI (27, 37).

Following this logic, we introduce a simple measure δ_{ij} to capture the level of asymmetry of a link connecting two nodes with degree k_i and k_j respectively, where $\delta_{ij} = (k_i - k_j)^2/(k_i + k_j)^2$. This measure produces values over the interval [0, 1], where $\delta_{ij} \equiv 1$ is a maximally asymmetric link, and is useful for comparisons because it rescales the absolute differences in degree. Looking at the empirical data to see how the frequency of refunds varies across links, we found a negative correlation between the asymmetry level of a link δ_{ij} and the probability of a refund occurring β_{ij}. This probability was calculated by a probit regression on δ_{ij} ($P < 0.001$) of the form $\beta(\delta_{ij}) = \frac{1}{1 + e^{-(a+b\delta_{ij})}}$, where $a = -0.832$ and $b = -1.11$ (see Fig. S8). The model was validated by the Homer–Lemeshow goodness-of-fit test with $P = 0.224$. This suggests that declining networks that favor asymmetric links increase the likelihood of preserving the network's functional relationships.

Generalized Model of Contraction

Guided by our empirical evidence, we constructed a simple model for network contraction that combines two main processes: asymmetric disassembly, which represents the contracting process, and PA, which represents the partial recovery process in our network (see Fig. S9 for a graphical representation of the model). In its general form, the model applies to undirected networks; however, an extension to directed networks is provided in *SI Text* and Figs. S10 and S11. The inputs for the model in each time step are the number of nodes deleted (DF) and created (NF), and the number of links deleted (DL) and created (NL) between incumbent nodes, all of which are given directly by the empirical data (see Table S3). The simulation model is initialized using the empirical network of 1985.

The first step in the model is motivated by the empirical observation that the network experiences a sustained net loss of firms each period. This generates the need for a rule on node deletion.

i. Node deletion is treated probabilistically with the inverse network connectivity providing a reasonable proxy for unob-

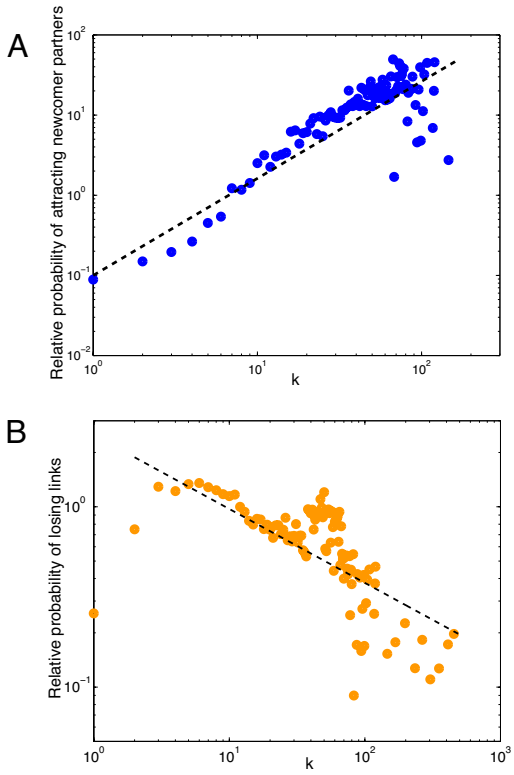

Fig. 2. Assembly and disassembly mechanisms. (*A*) Preferential attachment. Here, we considered the process by which links between incumbent and newcomer firms are created. Following Newman (39), the figure shows on a log-log scale the relative probability $T_k(t)$ that a newcomer firm added at time t connects to a incumbent firm with k previous connections. $T_k(t)$ is the ratio between the actual probability of connection and the probability of connection in a network where connectivity does not matter. The fit (dashed line) corresponds to the function $T_k(t) \sim k(t)^{\upsilon}$ with $\upsilon = 1.2$, which is a fair approximation to a linear preferential attachment giving the finite size of the network. The deviating points in the tail of the distribution all correspond to the idiosyncratic behavior of a single firm. (B) Link deletion. The figure shows on a log-log scale the relative probability of link deletion $R_k^-(t)$, compared with random link removal for each firm degree k. The dashed line corresponds to the function $k(t)^{\nu}$ with $\nu = -0.41$. Note that the least and the best connected firms are specially resistant to the loss of links. The data values are taken for the entire observation period whenever a firm survives for the following year. This gives ≈18,500 data points. Also note that if the calculated relative probabilities $T_k(t)$ and $R_k^-(t)$ were to follow a random process, $T_k(t) = 1$ and $R_k^-(t) = 1$ for all k values. The deviating points in the tail of the distribution correspond to the highly asymmetric connectivity of few high-degree firms that decreases their probability to losing links.

servable firm characteristics (e.g., age, size, etc.) that are known to determine survival rates. A node m is randomly selected and deleted from the LCC with a probability $P_{\text{delete}}(m) = k_m^{-1}/\Sigma_j k_j^{-1}$. The number of nodes deleted (DF) each time step is fixed empirically by the number of firms that do not appear in the dataset the following year and corresponds to ≈25% of the LCC.

The second step captures the fact that incumbent firms make two choices with respect to managing their links in each yearly production cycle: first, they can remove a link that connected them to a partner in the previous time period; second, they can replace a removed link with a connection to a new partner.

ii. Asymmetric disassembly and PA consists of removing and replacing links. For simplicity, we assume that links are randomly selected and are subjected to the following rules:

iia. Removing. In line with our empirical findings, selected links are removed with a probability defined by $p_{ij} = 1 - [(k_i - k_j)^2/(k_i + k_j)^2]$, which is given by the asymmetry level of the link. The number of links removed (DL) is taken from the empirical data as the interactions in a given year that do not recur in the following year, and corresponds approximately to 25% of the LCC.

iib. Replacing. For each link l_{ij} that is removed, one randomly chosen node (either i or j) replaces that link with probability q, otherwise both nodes lose the link. When replacing a link, the chosen node i or j selects a new node m following PA, with a probability $P(m) = (k_m + 1)/(\Sigma_j k_j + 1)$. The probability q was empirically fixed at $q = 0.9$, which corresponds to the average percentage of new links created between incumbent firms (NL/DL) over the entire observation period. Lower q values lead to a more rapid fragmentation of the network (see Fig. S12).

The third step corresponds to the creation of new links between newcomer and incumbent firms. This accounts for the parallel regrowth process observed in the network.

iii. PA growth characterizes how newcomer nodes are added to the network. The degree of each newcomer is taken from an exponential distribution with mean value 2, following our empirical findings (see Fig. S5). Newcomers link to an incumbent m following PA rules (4), defined by $P(m) = (k_m + 1)/(\Sigma_j k_j + 1)$. The number of nodes added (NF) each time step is given empirically by the new number of firms that appear in the dataset the following year, and corresponds approximately to 15% of the LCC.

Simulation Results and Discussion

Fig. 3*A–D* summarize the results. The data suggest that when the correct disassembly and assembly mechanisms are combined, the model accounts well for the empirically observed behavior and replicates the finding of topological robustness. We focus first on the recovery process. Fig. 3*A* shows the agreement between the actual empirical and model-generated values for the degree distribution when we use PA assembly mechanisms, as in the original model, and when we use random assembly mechanisms instead. Under random assembly, steps *iib* and *iii* of our model are modified so that incumbent and newcomer nodes attach to a randomly selected node m with probability $P(m) = 1/N$ where N is the total number of nodes in the LCC. As can be seen from the plot, different recovery rules are associated with distinct degree distributions. The PA assembly rules combined with asymmetric disassembly produce a high level of agreement with the empirically observed degree distribution for the contracting network.

Focusing on the contraction process as a whole, we compare the asymmetric disassembly process with three alternative mechanisms—random node deletion, random link removal and random assembly. Under random node deletion, step *i* of our model is modified so that nodes are selected and deleted with equal probability. For random link removal, step *iia* is modified so that the probability of link deletion is now given by $p_{ij} = 1$. Note as shown in Fig. 3*B*, that random link removal (red crosses) yields a flat distribution for the relative probability of link deletion $R_k^-(t)$ per node degree k. By contrast, asymmetric disassembly (blue circles) gives a good approximation to the empirical values shown in Fig. 2*B*. For the third alternative mechanism, random assembly, we replaced the PA assembly rules in steps *iib* and *iii* with random attachment as previously defined, $P(m) = 1/N$.

To test the network's robustness to fragmentation under each contraction mechanism, we measured the corresponding ratio between the model-generated number of nodes in the LCC and that of the empirical LCC. Fig. 3*C* shows that a contraction

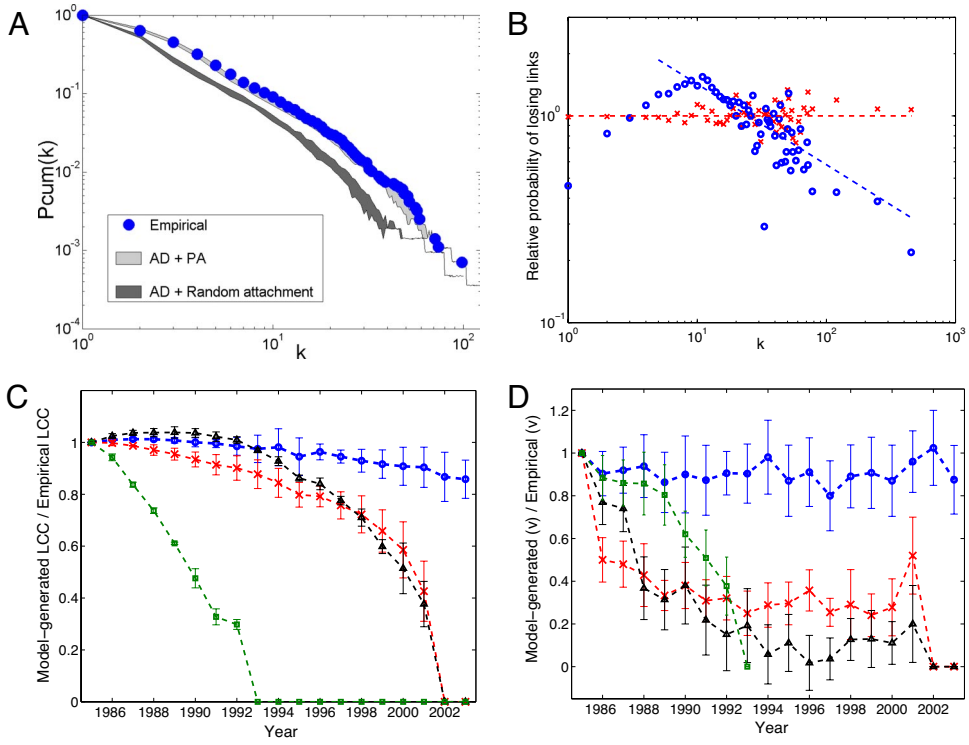

Fig. 3. Model validation. (*A*) Recovery mechanisms (1985–1987). Blue dots represent the empirical degree distribution in 1987. The gray region represents the 95% confidence intervals for the model-generated distribution in 1987 after asymmetric disassembly (AD) and PA recovery mechanisms in steps *iib* and *iii* of our model. The black region represents the 95% confidence intervals for the model-generated distribution in 1987 after asymmetric disassembly (AD) and random attachment recovery mechanisms. (*B*) Link removal. The figure shows the relative probability of link deletion $R_k^-(t)$ per node degree k after asymmetric disassembly (blue circles) and random link removal (red crosses). Fit to the data are shown by a dashed line defined by $k(t)^v$ with $v = -0.39 \pm 0.03$ ($R^2 = 0.64$) for asymmetric disassembly (blue circles) and $v = 0.011 \pm 0.002$ ($R^2 = 0.05$) for random deletion (red crosses). Note again that the deviating points in the tail of the distribution correspond to the highly asymmetric connectivity of few high-degree firms that decreases their probability to shedding links. (*C*) Network fragmentation. The figure shows the ratio (average ±2 SD) between the model-generated number of nodes in the LCC and that of the empirical LCC for each year after asymmetric disassembly (blue circles), random link removal (red crosses), random recovery (black triangles), and random node deletion (green squares). (*D*) Disassortativity. For the nearest-neighbor average connectivity defined by $\langle k_{nn} \rangle_k \sim k^v$, the figure shows the ratio (average ±2 SD) between the model-generated and empirical exponent v, when the network is subjected to asymmetric disassembly (blue circles), random link removal (red crosses), random recovery (black triangles), and random node deletion (green squares).

process that follows asymmetric disassembly (blue circles) best corresponds with the observed values over time, whereas random assembly (black triangles) and random link removal (red crosses) clearly do not reproduce the resistance to fragmentation of the LCC. Random node deletion (green squares) leads to an even faster network collapse.

Finally, we studied the network's robustness to topological changes generated by asymmetric disassembly and the three alternative contraction mechanisms. Fig. 3*D* shows for the nearest-neighbor average connectivity defined by $\langle k_{nn} \rangle_k \sim k^v$, the ratio between the model-generated and empirical exponent v. Note that only asymmetric disassembly (blue circles) is able to reproduce the observed disassortativity of the network (Fig. S13), and performs similarly well with important connectivity metrics such as the average path length and diameter of the network (see Fig. S14). These comparative results show that assembly and disassembly mechanisms have distinct effects on robustness.

Conclusions

Despite a large body of research on network growth, the complementary process of decline has been given short shrift. In both the case of growth and decline, a key issue is robustness. The specific network of firms in the NYGI that we have analyzed and modeled exhibits a remarkably robust topology and stable performance measures while undergoing severe decline. Ultimately the network collapses into a highly centralized configuration characterized by elevated error rates and reduced overall performance, suggesting the existence of a threshold of minimally functional connectivity.

At the microscopic level, the observed network robustness can be linked to the enhance functional and structural preference for asymmetric interactions. This result has an interesting counterpart in ecological network research on how species may be linked together (34) and respond to realistic extinction sequences (41). Our simulation studies enable us to extend our findings beyond the specific empirical context that we have focused on and show that alternative combinations of assembly and disassembly processes lead to a more rapid network fragmentation and changes in structural features. By augmenting studies of network growth with a general model of contraction and examining the consequences for topological robustness, we hope to open up new directions for research on network dynamics and robustness.

Methods

NYGI Dataset. This is longitudinal empirical dataset on the interfirm network of the New York City garment industry from 1985 to 2003. Our data include ≈700,000 transactions from January 1985 to December 2003 for 10,000 firms that collaborated in the production of clothing. A link exists between two firms if they coproduce a garment. For example, the typical production process begins with a designer that develops a line of clothing. Each garment in the line is made into a sample prototype, which is disassembled into its component parts such as shelves, collars, waistbands, and so forth. The components of the

sample are then sent by the designer to contractors that cut components from fabric in lots large enough to be mass produced. The cut fabric is then sent by the designer to sewing contractors that sew the fabric together into the garments that are sold directly to consumers at retailers. Links are typically undirected. Information and finances flow reciprocally as part of the production process, rather than directionally. That is, although the designer may produce the original design and sample prototype, the contractors in the network often add design changes that simplify production or enhance efficiency, which makes a final design a reciprocal effort. In our data, all designers and contractors are in the same finished goods stage of the production process; there are no downstream raw fabric suppliers (that only sell cloth) or upstream retailers (that only buy finished goods) in the data. All firms are free to make connections of their own choice; there is no governing body that suggests or mandates connections. Each transaction in the data are associated with a volume of exchange or a run. Because a single line of clothing is often produced in several runs, we aggregated runs between designers and contractors into a single link that represents the whole coproduction job. We focused on the largest connected component, which corresponds to 95% of the population. The dataset was collected and made available by the Union of Needle Trades and Industrial and Textile Employees (UNITE). UNITE organizes nearly all the firms in the NYGI and uses a highly reliable record system (27) that requires firms to report all their network contacts quarterly. These self-reports are checked by union auditors for accuracy. Nonunionized firms are typically small, fly-by-night firms that elude discovery because of their brief existence (27).

Network Performance. In the context of the NYGI, we acknowledge that error rates can fluctuate for various reasons. Based on prior research and personal communication with UNITE (43), we viewed errors as primarily due to the network's failure to govern effective collaborations among interdependent firms. However, error rates may occur for other reasons. For example, adverse selection could leave a biased sample of firms operating in the market or market power could enable some firms to force fake returns. On the basis of our data, we cannot fully discriminate between these different micro mechanisms. Nonetheless, these other factors seem unlikely. Firms that may be victimized can appeal to UNITE, which protects weak firms against abuses of market power. Similarly, with the onslaught of international competition, adverse selection seems unlikely in that the fittest firms are most likely to survive.

ACKNOWLEDGMENTS. We thank Mark Fricker, Neil Johnson, Janet Smart, and other colleagues in the CABDyN Complexity Centre (Oxford) and at Northwestern Institute on Complex Systems (Northwestern University) for helpful discussions and Paul David, Roger Guimerà, János Kertész, Bruce Kogut, Eduardo López, Avner Offer, Jukka-Pekka Onnela, Daniel Stouffer, Alex Vespignani and Peyton Young for comments on a previous draft. This work was supported by the Measuring and Modelling Complex Networks across Domains project, which is funded by the European Commission under the FP6 New and Emerging Science and Technology Pathfinder Initiative on ''Tackling Complexity in Science'' (F.R.-T.) and a Doctoral Research Studentship funded by Measuring and Modelling Complex Networks across Domains and Consejo Nacional de Ciencia y Tecnología (S.S.).

1. Albert R, Barabási AL (2002) Statistical mechanics of complex networks. *Rev Mod Phys* 74:47–97.
2. Newman MEJ (2003) The structure and function of complex networks. *SIAM Rev* 45:167–256.
3. Dorogovtsev SN, Mendes JFF (2005) *Evolution of Networks: From Biological Nets to the Internet and WWW* (Oxford Univ Press, Oxford).
4. Barabási AL, Albert R (1999) Emergence of scaling in random networks. *Science* 286:509–512.
5. Albert R, Barabási AL (2000) Topology of evolving networks: Local events and universality. *Phys Rev Lett* 85:5234–5237.
6. Bianconi G, Barabási AL (2001) Competition and multiscaling in evolving networks. *Europhys Lett* 54:436–442.
7. Solé RV, Pastor-Satorras R, Smith ED, Kepler TA (2002) A model of large-scale proteome evolution. *Adv in Complex Systems* 5:43–54.
8. Song C, Havlin S, Makse HA (2006) Origins of fractality in the growth of complex networks. *Nat Phys* 2:275–281.
9. Caldarelli G, Capocci A, De los Rios P, Munoz MA (2002) Scale-free networks from varying vertex intrinsic fitness. *Phys Rev Lett* 89:258702.
10. Park K, Lai Y-C, Ye N (2005) Self-organized scale-free networks. *Phys Rev E Stat Nonlin Soft Matter Phys* 72:026131.
11. Salathé M, May RM, Bonhoeffer S (2005) The evolution of network topology by selective removal. *J Roy Soc Interface* 2:533–536.
12. Moore C, Ghoshal G, Newman MRJ (2006) Exact solutions for models of evolving networks with addition and deletion of nodes. *Phys Rev E Stat Nonlin Soft Matter Phys* 74:036121.
13. Albert R, Jeong H, Barabási AL (2000) Error and attack tolerance of complex networks. *Nature* 406:378–382.
14. Cohen R, Erez K, ben-Avraham D, Havlin S (2000) Resilience of the Internet to random breakdowns. *Phys Rev Lett* 85:4626.
15. Holme P, Kim BJ, Yoon CN, Han SK (2002) Attack vulnerability of complex networks. *Phys Rev E Stat Nonlin Soft Matter Phys* 65:056109.
16. Wilson NR, Ty MT, Ingber DE, Sur M, Liu G (2007) Synaptic reorganization in scaled networks of controlled size. *J Neurosci* 27:13581–13589.
17. Pascual M, Dunne J, eds (2005) *Ecological Networks: Linking Structure to Dynamics in Food Webs* (Oxford Univ Press, Oxford).
18. Solé R, BascompteJ (2006) *Self-Organization in Complex Ecosystems* (Princeton Univ Press, Princeton).
19. Burt RS (2002) Bridge decay. *Soc Network* 24:333–363.
20. Kaivan M, Rosenzwieg M (2005) Economic development and the decline of rural and urban community based networks. *Econ Trans* 13:427–433.
21. May RM, Levin SA, Sugihara G (2008) Ecology for bankers. *Nature* 451:893–895.
22. Thadakamalla HR, Raghavan UN, Kumura S, Albert R (2004) Survivability of multiagent-based supply networks: A topological perspective. *IEEE Intelligent Syst* 19:24–31.
23. Grabher G, Stark D, eds (1997) *Restructuring Networks in Post-Socialism: Legacies, Linkages, and Localities* (Oxford Univ Press, Oxford).
24. David P (2005) Clio and the economics of QWERTY. *Am Econ Rev* 75:332–337.
25. Doeringer P, Crean S (2006) Can fast fashion save the apparel industry? *Socio-Econ Rev* 4:353–377.
26. US Department of Commerce and Bureau of the Census (1987–2002) *NY Economic Census Manufacturing* (U.S. Government Printing Office, Washington, DC).
27. B. Uzzi (1996) The sources and consequences of embeddedness for the economic performance of organizations: The network effect. *Am Sociological Rev* 61:674–698.
28. Serrano MA, Boguna M, Díaz-Guilera A (2003) Topology of the world trade web *Phys Rev E Stat Nonlin Soft Matter Phys* 68:015101.
29. Söramaki K, Bech ML, Arnold J, Glass RJ, Beyeler WE (2007) The topology of interbank payment flows (2007) *Physica A* 379:317–333.
30. Garlaschelli D, Di Matteo T, Aste T, Caldarelli G, Loffredo MI (2007) Interplay between topology and dynamics in the World Trade Web. *Eur Phys J B* 57:159–164.
31. Hidalgo CA, Klinger B, Barabási AL, Hausmann R)2007) The product space conditions the development of nations. *Science* 317:482–487.
32. Vázquez A, Pastor-Satorras R, Vespignani A (2002) Large-scale topological and dynamical properties of the Internet. *Phys Rev E Stat Nonlin Soft Matter Phys* 65:066130.
33. Maslov S, Sneppen K (2002) Specificity and stability in topology of protein networks. *Science* 296:910–913.
34. Bascompte J, Jordano P, Olesen JM (2006) Asymmetric coevolutionary networks facilitate biodiversity maintenance. *Science* 312:431–433.
35. Powell WW, White DR, Koput KW, Owen-Smith J (2003) Network dynamics and field evolution: The growth of interorganizational collaboration in the life sciences. *Am J Soc* 110:1132–1205.
36. Moody J (2004) The structure of social science collaboration network: Disciplinary cohesion from 1963–1999. *Am Soc Rev* 69:213–238.
37. Podolny JM (2005) *Status Signals: A Sociological Study of Market Competition* (Princeton Univ Press, Princeton).
38. Merton RK (1968) The Matthew effect in science. *Science* 159:56–63.
39. Newman MEJ (2001) Clustering and preferential attachment in growing networks *Phys Rev E Stat Nonlin Soft Matter Phys* 64:025102.
40. Lehmann S, Jackson AD, Lautrup B (2005) Life, death and preferential attachment. *Europhys Lett* 69:298–303.
41. Srinivasan UT, Dunne JA, Harte J, Martinez ND (2007) Response of complex food webs to realistic extinction sequences. *Ecology* 88:671–682.
42. Newman MEJ (2005) Power laws, Pareto distriibutions and Zipf's law *Contemporary Phys* 46:323–351.
43. Waldinger R (1986) *Through the Eye of the Needle: Immigrants and Enterprise in New York's Garment Trades* (New York Univ Press, New York).